

SUPPLEMENTARY MATERIAL

Ru-based nanoparticles supported on carbon nanotubes for electrocatalytic hydrogen evolution: structural and electronic effects

Nuria Romero,^{a,b*,&} Dídac A. Fenoll,^{a,&} Laia Gil,^a Sergi Campos,^a Jordi Creus,^{a,b} Gerard Martí,^a Javier Heras-Domingo,^a Vincent Collière,^b Camilo A. Mesa,^c Sixto Giménez,^c Laia Francàs,^a Luis Rodríguez-Santiago,^a Xavier Solans-Monfort,^{a*} Mariona Sodupe,^a Roger Bofill,^a Karine Philippot,^{b*} Jordi García-Antón,^a and Xavier Sala^{a*}

^a Departament de Química, Universitat Autònoma de Barcelona, 08193 Bellaterra (Cerdanyola del Vallès), Catalonia (Spain). E-mail: xavier.sala@uab.cat, xavier.solans@uab.cat

^b CNRS, LCC (Laboratoire de Chimie de Coordination), UPR8241, Université de Toulouse, UPS, INPT, F-31077 Toulouse cedex 4, France. E-mail: nuria.romero@lcc-toulouse.fr, karine.philippot@lcc-toulouse.fr

^c Institute of Advanced Materials (INAM), Universitat Jaume I, Avenida de Vicente Sos Baynat, s/n, 12006 12006 Castelló de la Plana, Castellón, Spain.

* Corresponding authors

& These authors contributed equally to this work.

List of Contents

page

1. Electron microscopy characterization of the hybrid nanomaterials	3
2. HER catalytic studies of the hybrid nanomaterials	7
3. Computational studies	11

1. Electron microscopy characterization of the hybrid nanomaterials

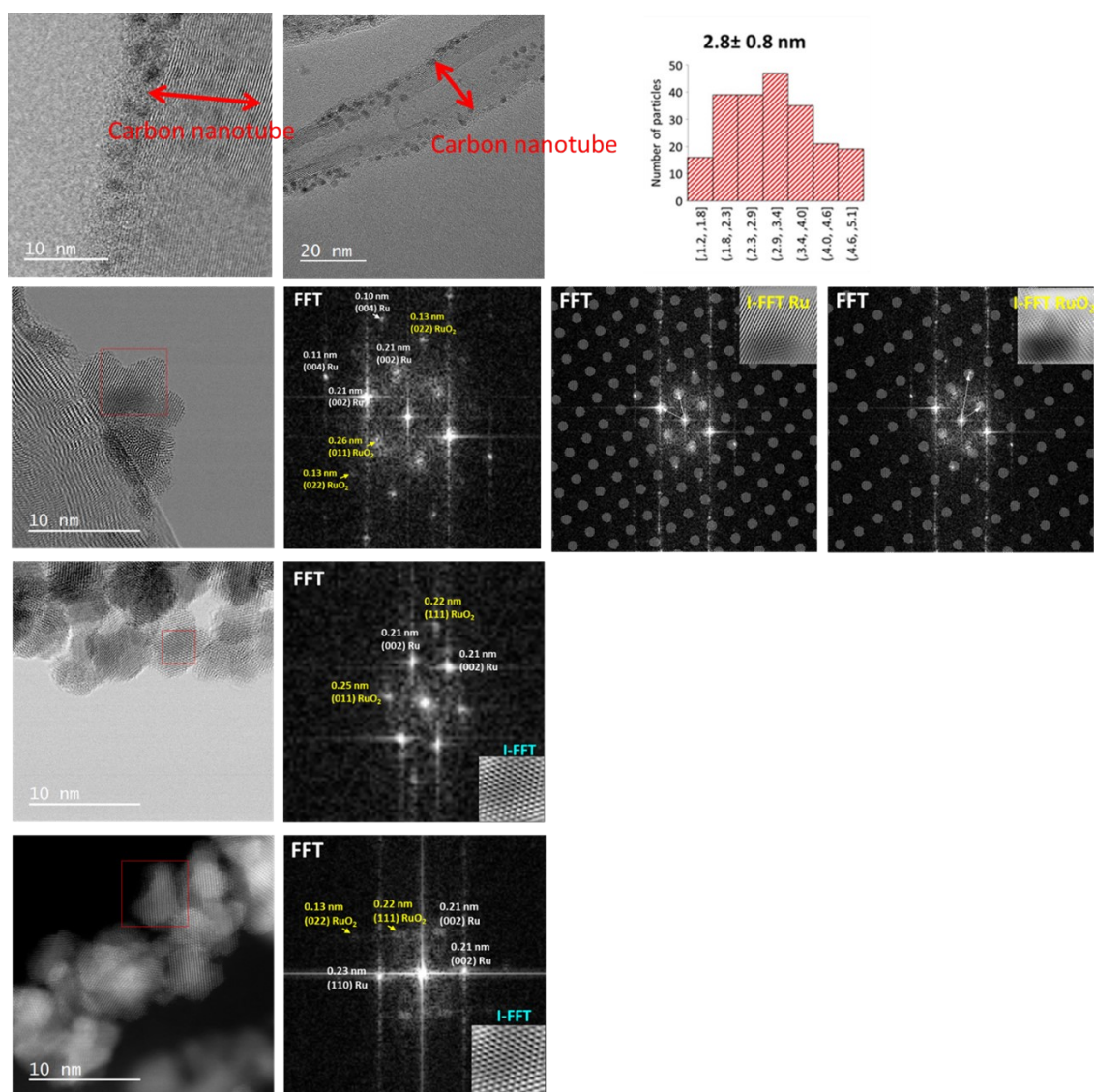


Figure S1. HRTEM images and size histogram of the Ru@RuO₂/CNT nanomaterial, including electron diffraction patterns after Fast Fourier Transform treatment of individual nanoparticles (on a holey carbon covered Cu grid).

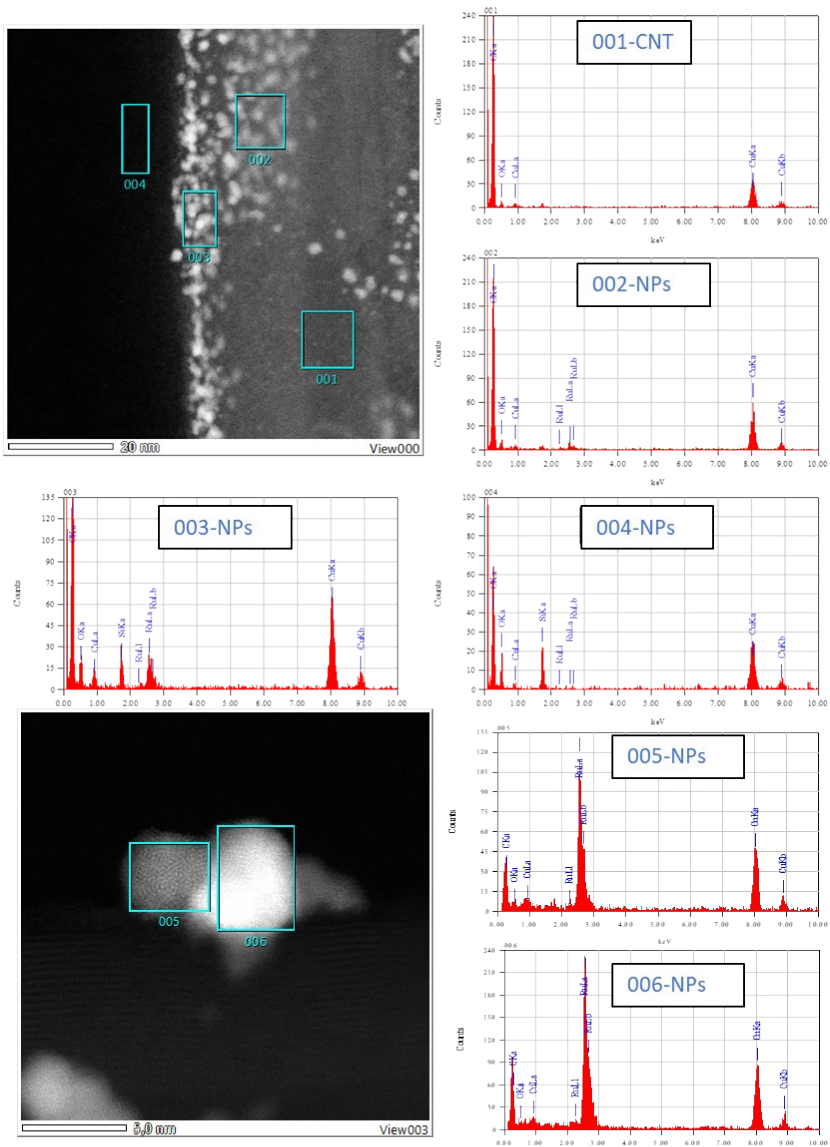


Figure S2. EDX spectra on different regions of HRTEM images of Ru@RuO₂/CNT: general EDX analysis (top) and nanoparticle analysis (bottom, holy carbon covered Cu grid).

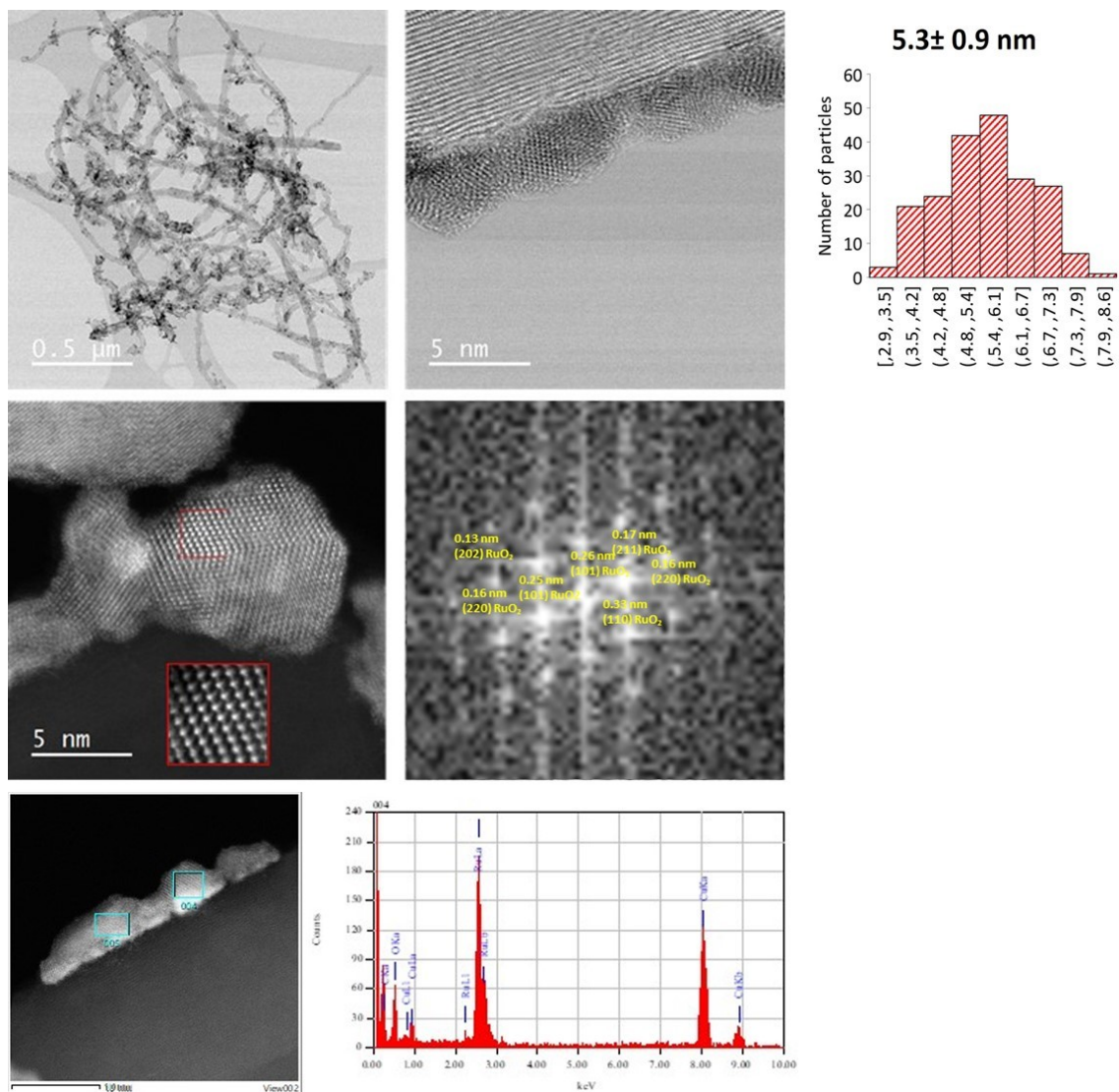


Figure S3. TEM and HRTEM images, NPs size histogram, FFT pattern and EDX analysis of the RuO₂-10'/CNT nanomaterial.

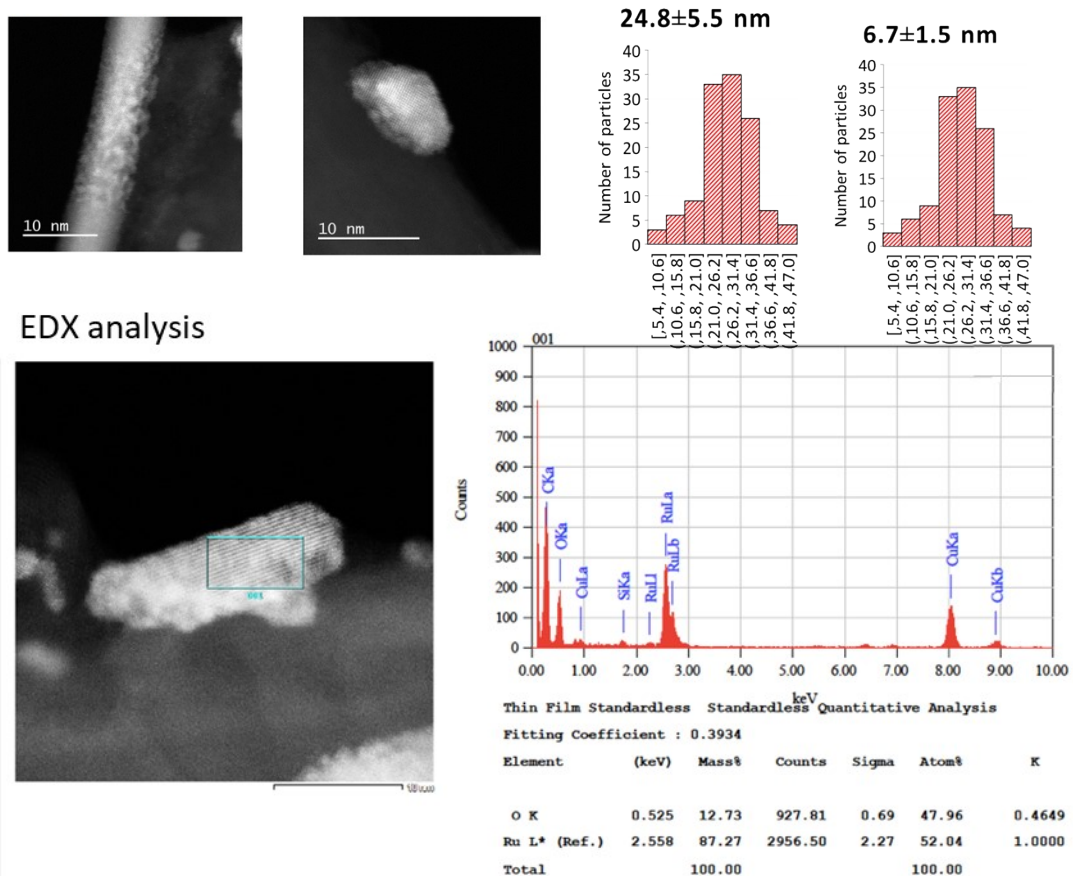


Figure S4. TEM and HRTEM images, NPs size histogram and EDX analysis of the **RuO₂-120'/CNT** nanomaterial.

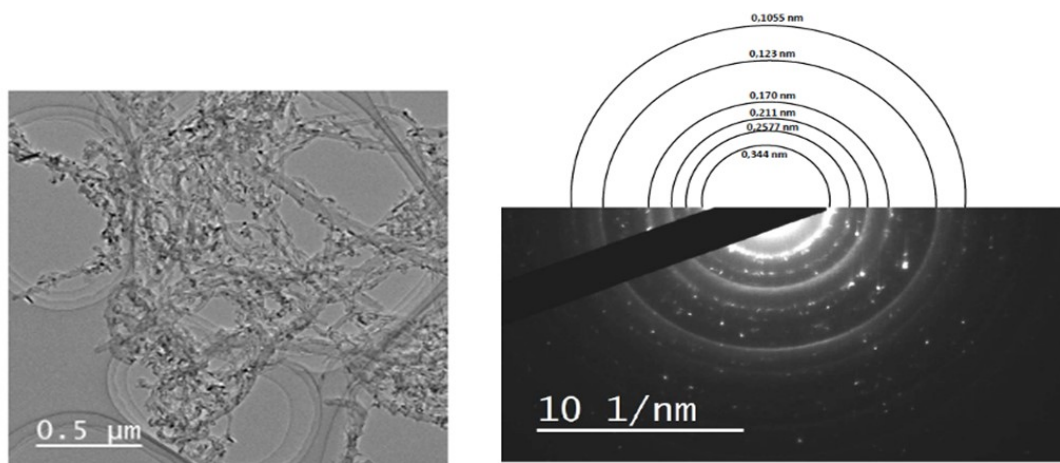


Figure S5. Electron diffraction analysis of a large zone of the **RuO₂-120'/CNT** nanomaterial.

2. HER catalytic studies of the hybrid nanomaterials

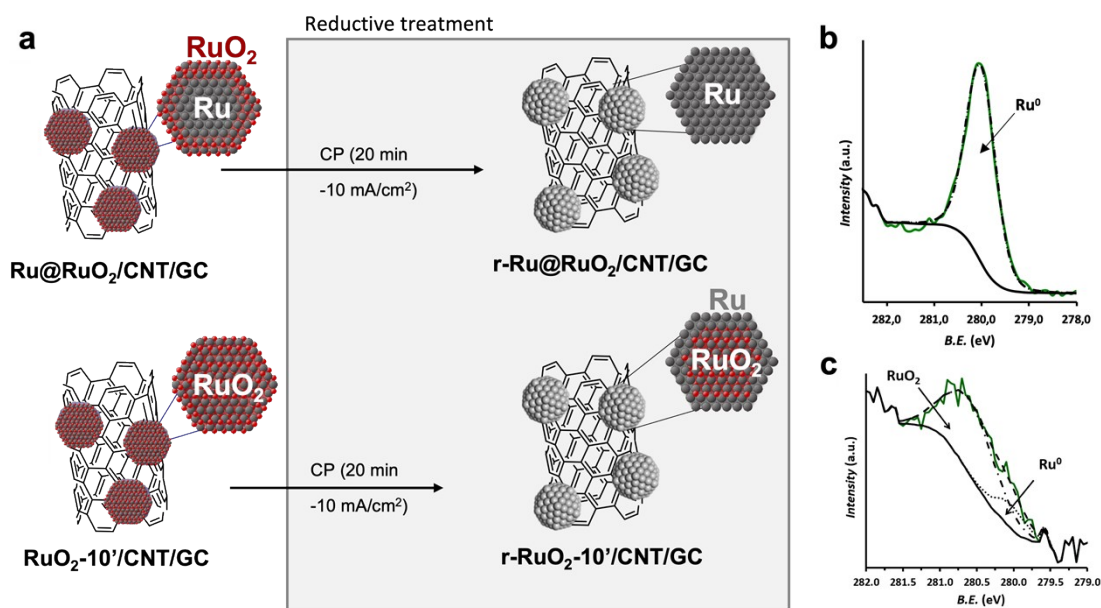


Figure S6. (a) Scheme of the chronopotentiometry reductive treatment applied to the GC RDE deposited nanomaterials, leading to their reduced counterparts. (b) XPS spectrum of **r-Ru@RuO₂/CNT/GC** and (c) XPS spectrum of **r-RuO₂-10'/CNT/GC**. The RuO₂ component is shown in dotted-dashed black, the Ru(0) component in dotted black, the envelope in dashed black, the experimental data in solid green and the background signal in solid black.

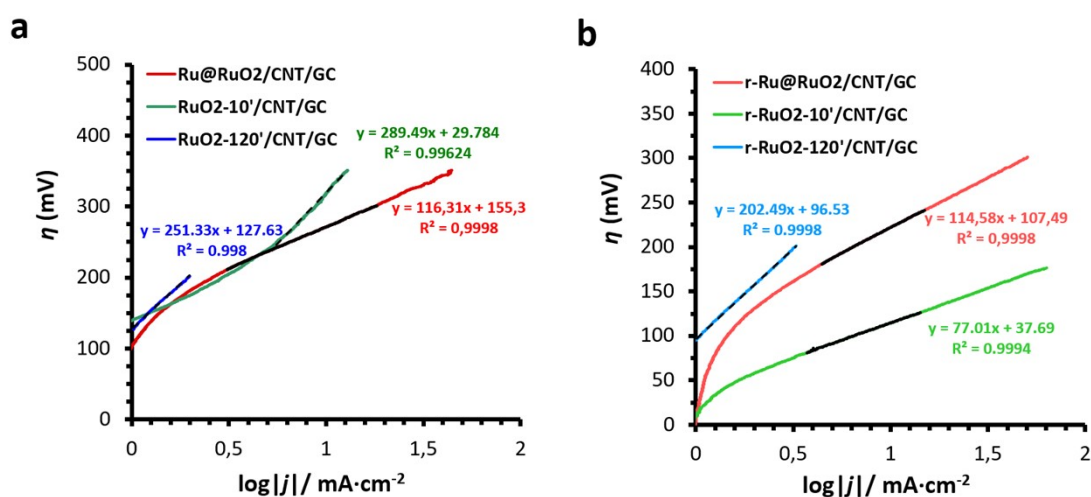


Figure S7. Tafel plots in 1 M H₂SO₄ corresponding to the HER process of **Ru@RuO₂/CNT/GC** (red), **RuO₂-10'/CNT/GC** (green) and **RuO₂-120'/CNT/GC** (blue) (a), and of their reduced counterparts, **r-Ru@RuO₂/CNT/GC** (orange), **r-RuO₂-10'/CNT/GC** (light green) and **r-RuO₂-120'/CNT/GC** (light blue) after a 20 min reductive chronopotentiometry at $j = -10 \text{ mA}\cdot\text{cm}^{-2}$ (b).

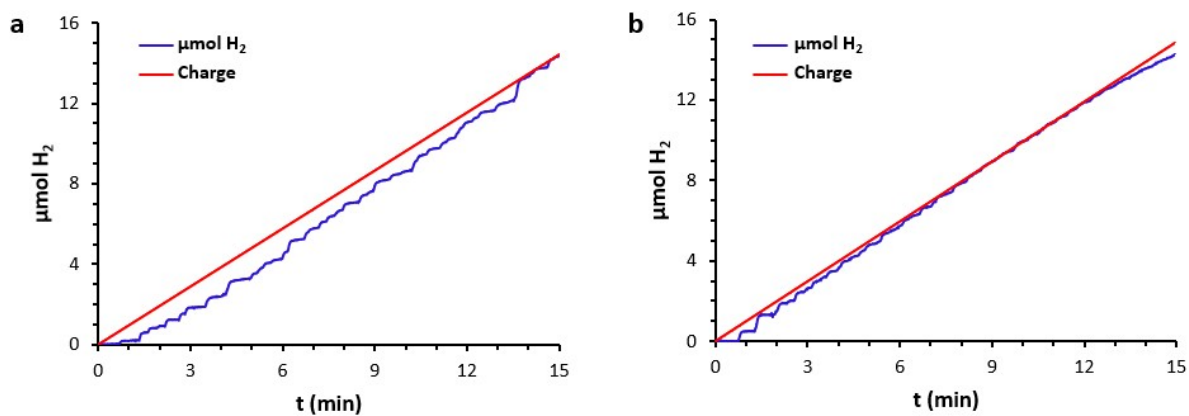


Figure S8. H₂ measurement during a reductive CP at -10 mA·cm⁻² for r-Ru@RuO₂/CNT/FTO (a), and r-RuO₂-10'/CNT/FTO, (b), in 1 M H₂SO₄.

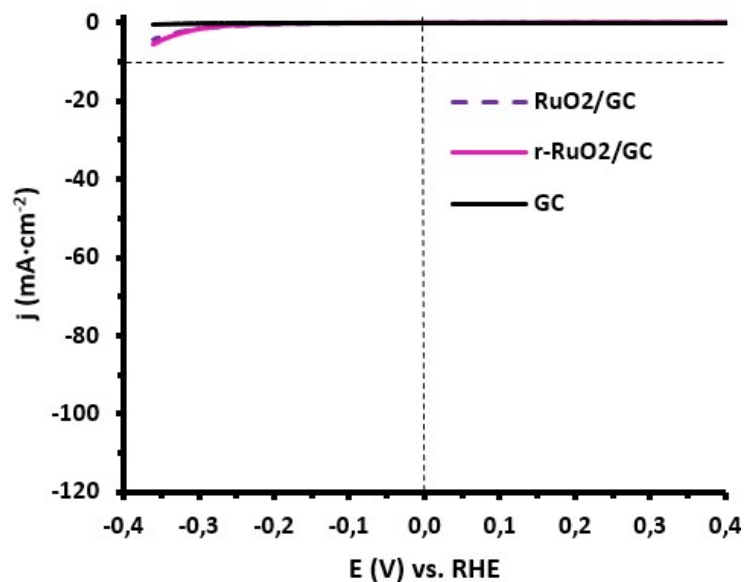


Figure S9. LSVs in 1 M H₂SO₄ of bulk commercial RuO₂/GC (dashed purple), r-RuO₂/GC (solid pink) and the bare GC electrode (solid black). The thermodynamic HER potential in 1 M H₂SO₄ and the reference $j = -10 \text{ mA}\cdot\text{cm}^{-2}$ current density are indicated as black dashed lines.

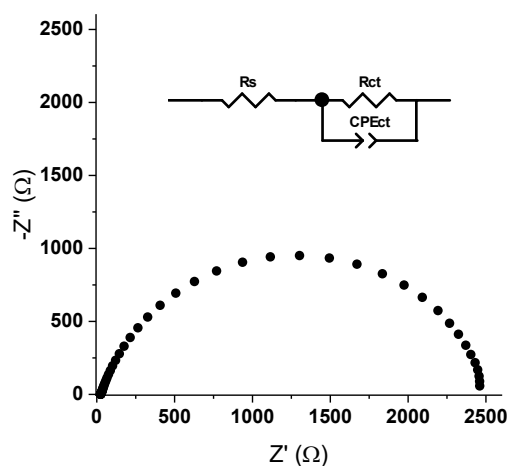


Figure S10. Typical Nyquist obtained for the electrodes studied herein. Nyquist plot of **CNT/GC** measured at -0.3 V vs NHE. Inset: Randles circuit employed to fit the experimental data.

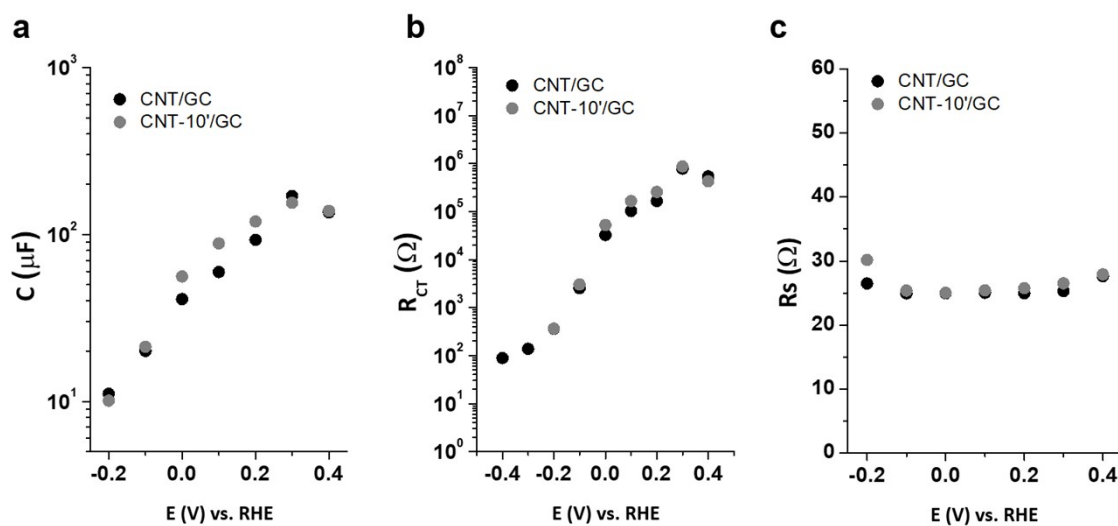


Figure S11. Impedance spectroscopy results C , R_1 and R_s , fitting the Nyquist plots to a simple Randles circuit of **CNT/GC** (black) and **CNT-10'/GC** (dark grey). (a) Capacitance (C), (b) charge transfer resistance (R_{CT}) and (c) series resistance (R_s).

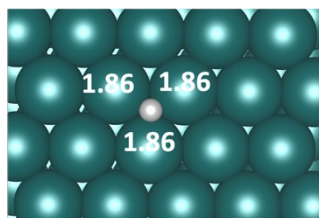
Table S1. Main physicochemical and electrochemical data of the CNT-supported Ru-based nanomaterials for HER in 1 M H₂SO₄.

Entry	System	NP mean size (nm)	NP composition	η_0 (mV)	η_{10} (mV)	b (mV·dec⁻¹)
1	Ru@RuO₂/CNT/GC	2.8 ± 0.8	Ru ⁰ /RuO ₂ core/shell	200	272	116
2	r-Ru@RuO₂/CNT/GC ⁱ	---	Ru ⁰ ⁱⁱ	150	222	115
3	RuO₂-10'/CNT/GC	5.3 ± 0.9	RuO ₂	130	319	289
4	r-RuO₂-10'/CNT-/GC ⁱ	---	RuO ₂ /Ru ⁰ core/shell	50	115	77
5	RuO₂-120'/CNT/GC	Nanorods: broad (6.7 ± 1.5 nm) and long (24.8 ± 5.5 m) crystals	RuO ₂	125	-	251
6	r-RuO₂-120'/CNT/GC ⁱ	---	RuO ₂	95	-	202

ⁱ These nanomaterials were treated under chronopotentiometry reductive conditions ($j = -10$ mA·cm⁻²) for 20 min. ⁱⁱ The oxidation state is assumed on the basis of literature data (ref. 5).

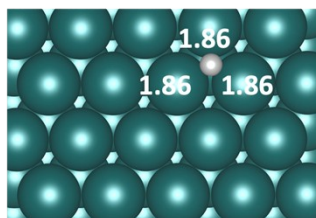
3. Computational studies

$$\theta = 1/N$$



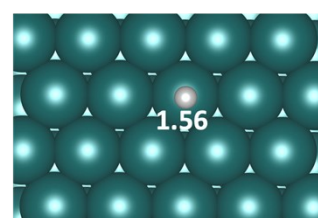
-58.0

3_{Oh}



-52.4

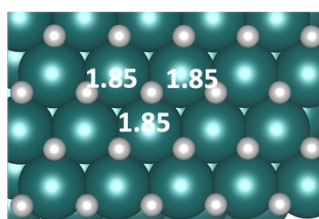
3_{Td}



-56.3

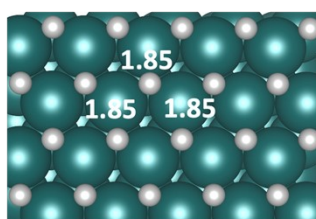
1_{Top}

$$\theta = 1$$



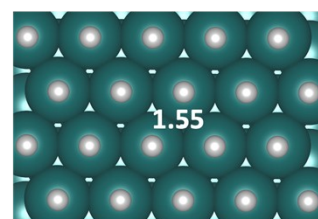
-49.5

3_{Oh}



-44.1

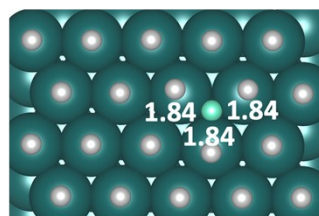
3_{Td}



-50.3

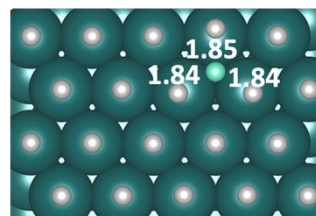
1_{Top}

$$\theta = (N+1)/N$$



-32.0

M-3_{Oh}



-34.9

M-3_{Td}

Figure S12. Optimized structures and adsorption energies for hydrogen onto a Pt surface as a function of the coverage. The additional hydrogen in the $\theta = 1$ coverage is represented in pale green. Pt-H distances are in Å and energies in $\text{kJ}\cdot\text{mol}^{-1}$.

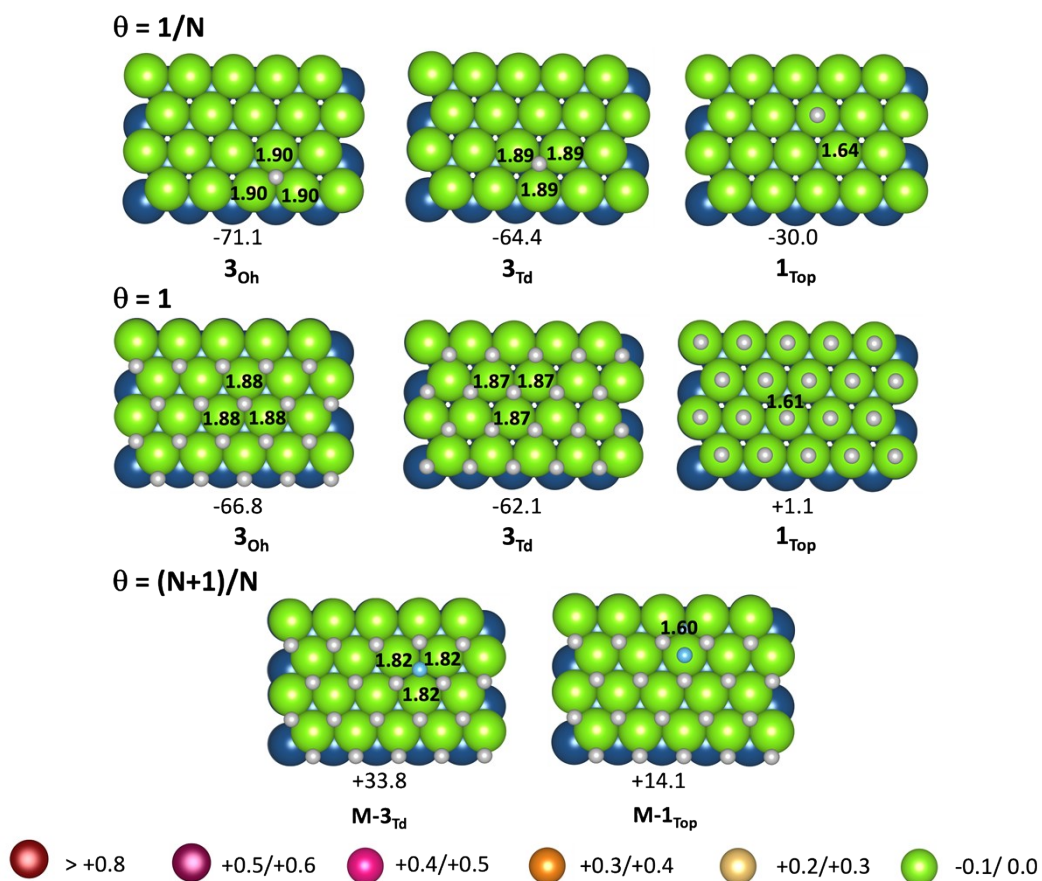


Figure S13. Optimized structures and adsorption energies for hydrogen onto a **Ru** surface as a function of the coverage. The additional hydrogen in the $\theta = 1$ coverage is represented in pale blue. The outermost atom color labeling indicates the atomic Bader charges of the pristine material. Ru-H distances are in Å and energies in $\text{kJ}\cdot\text{mol}^{-1}$.

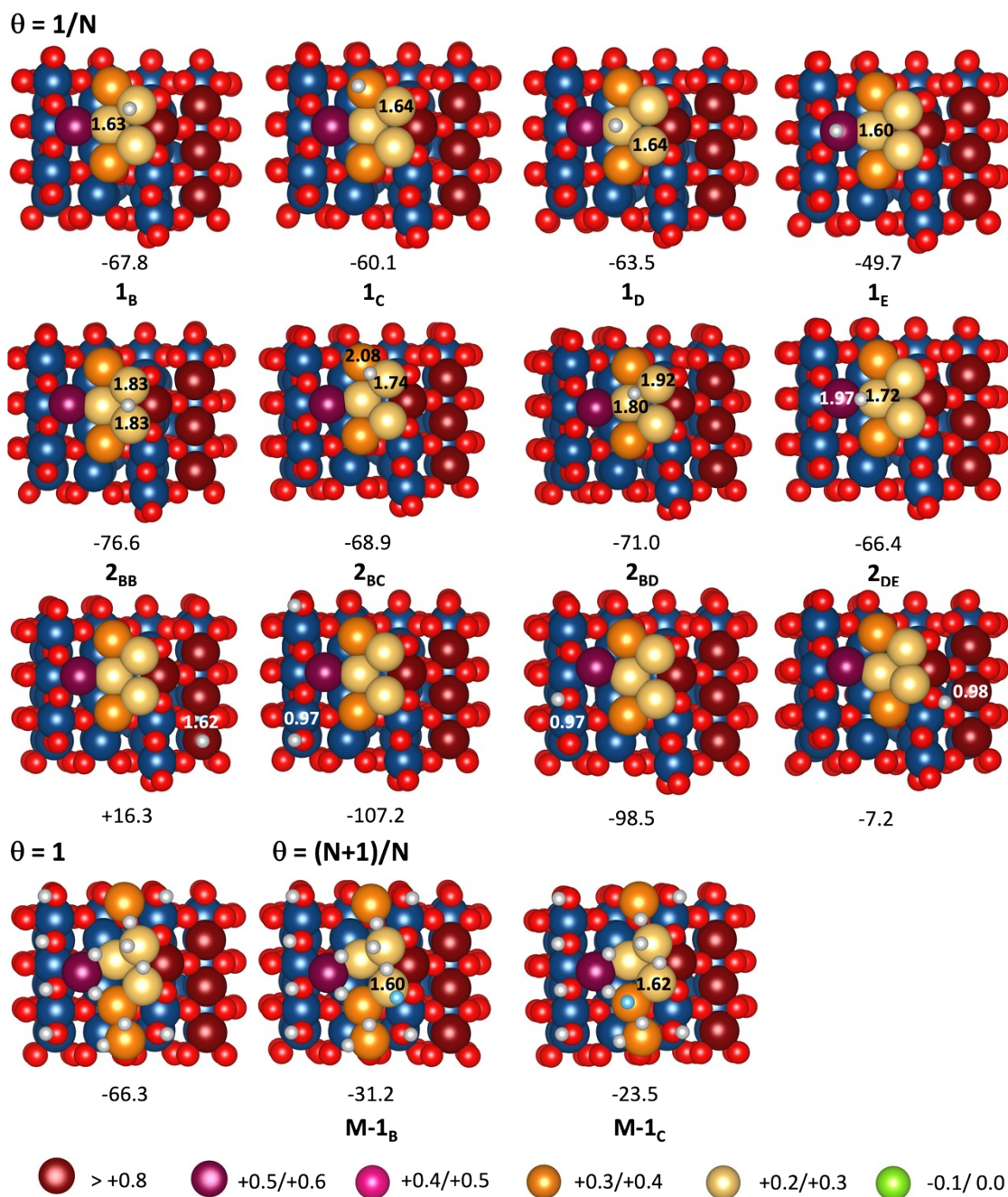


Figure S14. Optimized structures and adsorption energies for hydrogen onto a $\text{RuO}_2@\text{Ru}_7$ model of $r\text{-RuO}_2\text{-10'}/\text{CNT}/\text{GC}$ as a function of the coverage. The additional hydrogen in the $\theta = 1$ coverage is represented in pale blue. The outermost atom color labeling indicates the atomic Bader charges of the pristine material. Ru-H distances are in Å and energies in $\text{kJ}\cdot\text{mol}^{-1}$.

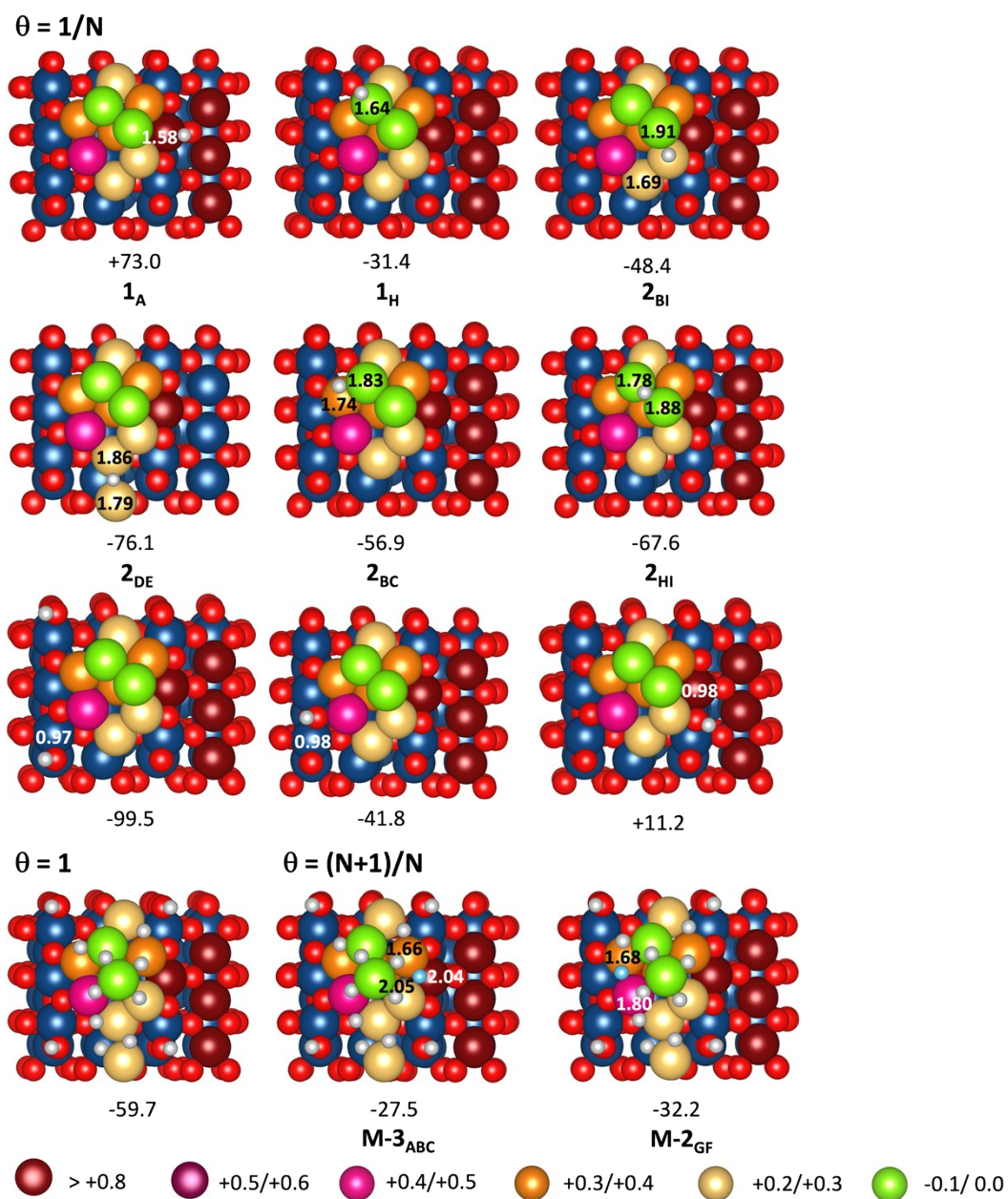


Figure S15. Optimized structures and adsorption energies for hydrogen onto a $\text{RuO}_2@Ru_{10}$ model of $r\text{-RuO}_2\text{-10'}/\text{CNT}/\text{GC}$ as a function of the coverage. The additional hydrogen in the $\theta = 1$ coverage is represented in pale blue. The outermost atom color labeling indicates the atomic Bader charges of the pristine material. Ru-H distances are in Å and energies in $\text{kJ}\cdot\text{mol}^{-1}$.

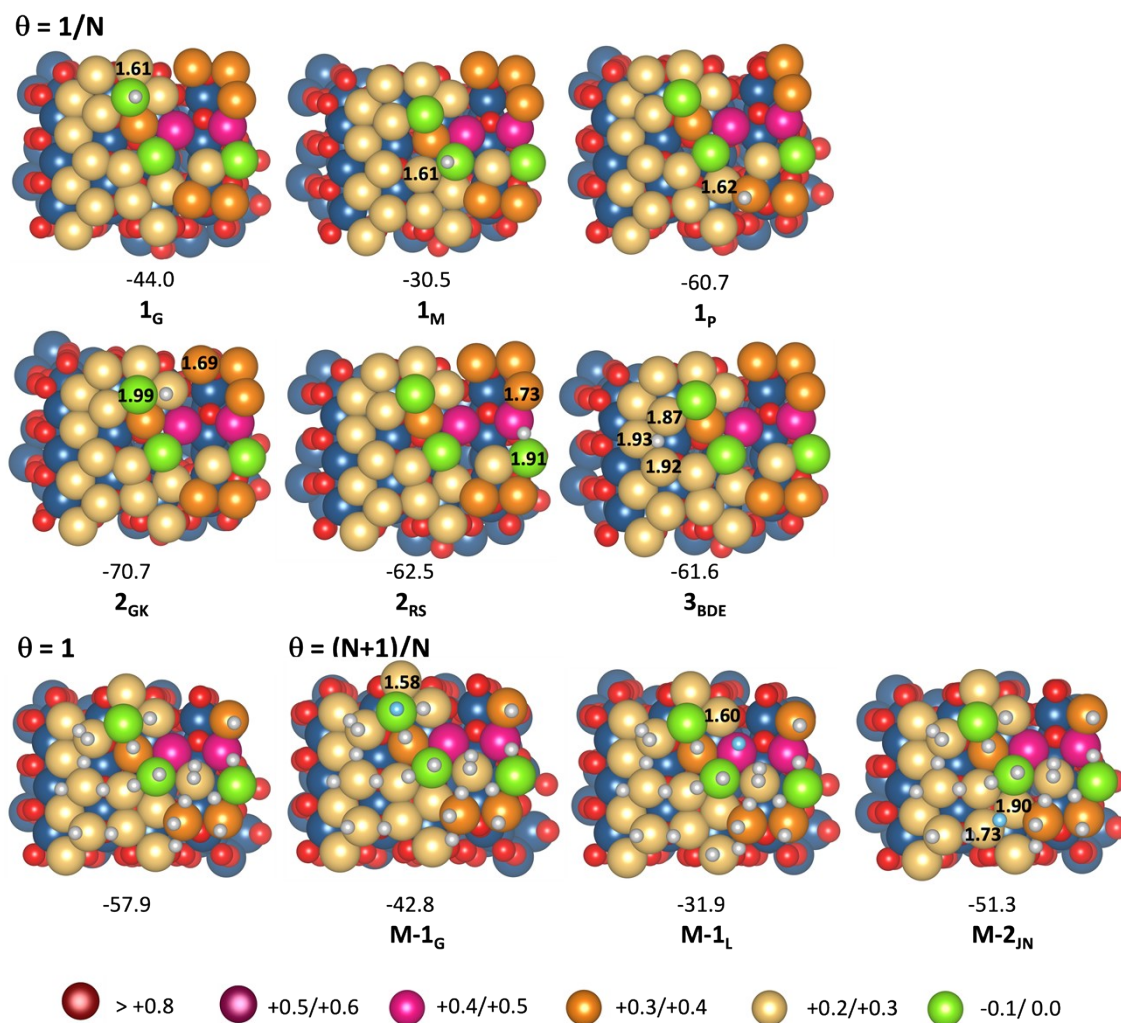
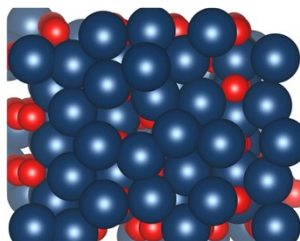


Figure S16. Optimized structures and adsorption energies for hydrogen onto a $\text{RuO}_2@Ru_{20}$ model of $r\text{-RuO}_2\text{-10'}/\text{CNT}/\text{GC}$ as a function of the coverage. The additional hydrogen in the $\theta = 1$ coverage is represented in pale blue. The outermost atom color labeling indicates the atomic Bader charges of the pristine material. Ru-H distances are in \AA and energies in $\text{kJ}\cdot\text{mol}^{-1}$.

Top view



Side view

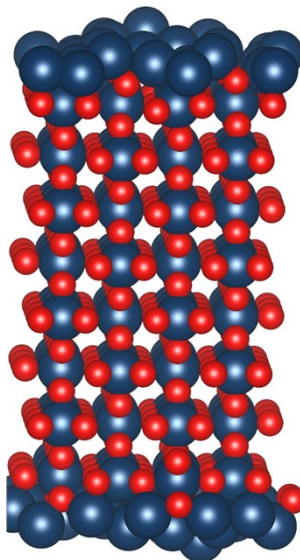


Figure S17. RuO₂@Ru₂₀ model including eight RuO₂ layers in the core.